

A COMPARISON OF DIRECT SOLVERS IN FROSch APPLIED TO CHEMO-MECHANICS

Alexander Heinlein*, Bjoern Kiefer†, Stefan Prüger†, Oliver Rheinbach^{◇△} and Friederike Röver[△]

*Delft University of Technology
Delft Institute of Applied Mathematics
Mekelweg 4, 2628 CD Delft, Netherlands
e-mail: a.heinlein@tudelft.nl

†Technische Universität Bergakademie Freiberg
Institute of Mechanics and Fluid Dynamics
Lampadiusstr. 4, 09599 Freiberg, Germany
e-mail: {Bjoern.Kiefer, Stefan.Prueger}@imfd.tu-freiberg.de

◇Technische Universität Bergakademie Freiberg
Institut für Numerische Mathematik und Optimierung; also Center for Efficient High Temperature Processes and Materials Conversion (ZeHS), and University Computing Center (URZ)
Akademiestr.6, 09599 Freiberg, Germany
e-mail: Oliver.Rheinbach@math.tu-freiberg.de

△Technische Universität Bergakademie Freiberg
University Computing Center (URZ)
Bernhard-v.-Cotta Str. 1, 09599 Freiberg, Germany
e-mail: Friederike.Roever@hrz.tu-freiberg.de

Key words: Chemo-Mechanics, Domain Decomposition, Overlapping Schwarz, Preconditioner, Trilinos, FROSch, Deal.II

Abstract. Sparse direct linear solvers are at the computational core of domain decomposition preconditioners and therefore have a strong impact on their performance. In this paper, we consider the Fast and Robust Overlapping Schwarz (FROSch) solver framework of the Trilinos software library, which contains a parallel implementations of the GDSW domain decomposition preconditioner. We compare three different sparse direct solvers used to solve the subdomain problems in FROSch. The preconditioner is applied to different model problems; linear elasticity and more complex fully-coupled deformation diffusion-boundary value problems from chemo-mechanics. We employ FROSch in fully algebraic mode, and therefore, we do not expect numerical scalability. Strong scalability is studied from 64 to 4096 cores, where good scaling results are obtained up to 1728 cores. The increasing size of the coarse problem increases the solution time for all sparse direct solvers.

1 FROSch preconditioner framework

Domain decomposition preconditioners are suitable for parallel computations, since they decompose, based on the computational domain, the problem into smaller subdomain problems,

which can be solved in parallel. In this paper, we consider the Fast and Robust Overlapping Schwarz (FROSch) preconditioner framework [12] of the Trilinos software library [2]. The framework contains a parallel implementation of the Generalized-Dryja-Smith-Widlund (GDSW) preconditioner [8]. The GDSW preconditioner is a two-level overlapping Schwarz preconditioner [19] with an energy-minimizing coarse space, which can be written in the form

$$M_{\text{GDSW}}^{-1} = \Phi K_0^{-1} \Phi^T + \sum_{i=1}^N R_i^T K_i^{-1} R_i. \quad (1)$$

Here, $K_i = R_i K R_i^T$, $i = 1, \dots, N$, represent the local subdomain problems on the overlapping subdomain Ω'_i , which we solve using a sparse direct solver. Each overlapping subdomain Ω'_i is obtained by recursively adding layers of elements to the nonoverlapping subdomain Ω_i . The global coarse problem $K_0 = \Phi^T K \Phi$ is solved using a sparse direct solver as well. The matrix Φ contains the coarse basis functions, as columns, spanning the global coarse space. For the construction of the GDSW coarse space functions, we consider interface functions Φ_Γ of the nonoverlapping decomposition. The interface functions are chosen as restrictions of the null space of the global Neumann matrix to the interface components, such as the vertices, edges and in 3D faces. We obtain the global coarse basis functions Φ by energy minimizing extensions of Φ_Γ into the interior of the nonoverlapping subdomain Ω_i . We obtain

$$\Phi = \begin{bmatrix} -K_{II}^{-1} K_{I\Gamma} \Phi_\Gamma \\ \Phi_\Gamma \end{bmatrix}. \quad (2)$$

For scalar elliptic problems and regular decompositions the GDSW preconditioner has a known condition number bound

$$\kappa(M_{\text{GDSW}}^{-1} K) \leq C \left(1 + \frac{H}{\delta}\right) \left(1 + \log\left(\frac{H}{h}\right)\right), \quad (3)$$

where C is a constant independent of the problem parameters, h the element, H the subdomain size and δ the subdomain overlap; cf. [9, 8]. For extended parallel scalability, the FROSch framework includes an implementation of the reduced dimensional GDSW (RGDSW) coarse space [10] as well as a multi-level extension [14]. However, for all results presented here, we only applied the classical GDSW coarse space and two levels.

2 Model problems

2.1 Linear elasticity

As a first model problem, we consider the linear elasticity model problem in three dimensions: find $\mathbf{u} \in H^1(\Omega)^3$

$$\begin{aligned} -\operatorname{div}(\boldsymbol{\sigma}) &= f && \text{in } \Omega \\ \mathbf{u} &= 0 && \text{on } \partial\Omega_D \end{aligned} \quad (4)$$

We use a generic right-hand-side vector of ones $(1 \dots 1)^T$ and use the standard implementations from [15] based on [1].

2.2 Coupled mechanics-diffusion problems

In contrast to the linear boundary value problem introduced in section 2.1, the model considered in this section incorporates material and geometrically nonlinear effects in a fully coupled formulation of the mechanical balance of momentum and Fickian diffusion. The model employs the rate-type potential from [5],

$$\Pi(\dot{\boldsymbol{\varphi}}, \dot{v}, \mathbf{J}_v) = \frac{d}{dt} \underbrace{\int_{\mathcal{B}} \hat{\psi}(\nabla \boldsymbol{\varphi}, v) dV}_{E(\boldsymbol{\varphi}, v)} + \underbrace{\int_{\mathcal{B}} \hat{\phi}(\mathbf{J}_v; \nabla \boldsymbol{\varphi}, v) dV}_{D(\mathbf{J}_v)} - P_{\text{ext}}^{\varphi}(\dot{\boldsymbol{\varphi}}) - P_{\text{ext}}^{\mu}(\mathbf{J}_v), \quad (5)$$

in which E denotes the stored energy functional, depending on the deformation $\boldsymbol{\varphi}$ through its material gradient and the swelling volume fraction v . Furthermore, the dissipation potential functional D associated with the body \mathcal{B} is a function of the fluid flux \mathbf{J}_v and is additionally parameterized by means of the deformation gradient and the swelling volume fraction. The mechanical part of the external load functional, associated volumetric body forces and prescribed tractions, is abbreviated with P_{ext}^{φ} , whereas P_{ext}^{μ} expresses the corresponding diffusion part, which depends upon the normal component of fluid flux, i.e. $H_v = \mathbf{J}_v \cdot \mathbf{N}$. By incorporating the balance of solute volume

$$\dot{v} = -\text{Div}[\mathbf{J}_v] \quad (6)$$

in (5), the primary fields can be computed from the two-field minimization principle

$$\{\dot{\boldsymbol{\varphi}}, \mathbf{J}_v\} = \text{Arg} \left\{ \inf_{\dot{\boldsymbol{\varphi}} \in \mathcal{W}_{\dot{\boldsymbol{\varphi}}}} \inf_{\mathbf{J}_v \in \mathcal{W}_{\mathbf{J}_v}} \Pi(\dot{\boldsymbol{\varphi}}, \mathbf{J}_v) \right\}, \quad (7)$$

in which the following admissible function spaces are chosen:

$$\begin{aligned} \mathcal{W}_{\dot{\boldsymbol{\varphi}}} &= \{ \dot{\boldsymbol{\varphi}} \in H^1(\mathcal{B}) \mid \dot{\boldsymbol{\varphi}} = \dot{\boldsymbol{\varphi}} \text{ on } \partial \mathcal{B}^{\varphi} \}, \\ \mathcal{W}_{\mathbf{J}_v} &= \{ \mathbf{J}_v \in H(\text{Div}, \mathcal{B}) \mid \mathbf{J}_v \cdot \mathbf{N} = H_v \text{ on } \partial \mathcal{B}^{H_v} \}. \end{aligned} \quad (8)$$

In the implementation of this model, a free-energy function ψ of Neo-Hookean type in connection with a Flory-Rehner type energy that accounts for the energy due to changes in the swelling volume fraction, and a quadratic dissipation potential ϕ are chosen. Upon the application of the Euler backward time integration to (6) and (5), the time discrete counterpart of (7) is employed to compute the primary fields $\boldsymbol{\varphi}|_{n+1}$ and $\mathbf{J}_v|_{n+1}$ at time t_{n+1} . Note that the employed variational principle ensures that the linearization of the necessary optimality condition yields a symmetric system of equations. For more details, the interested reader is referred to [17, 5]. The following specific model problems were also used in [17].

2.2.1 Free-swelling boundary value problem

This problem was also investigated in [17]. In the free-swelling boundary value problem, a cube of edge length $2L$, as shown in Figure 1(a), is considered. It is loaded in terms of a temporarily varying fluid flux at the outer boundary, while the outer surface remains traction free. Due to the intrinsic symmetry of the problem, only one eighth of the cube is taken into account in the scalability studies. Therefore, appropriate symmetry boundary conditions are applied along the symmetry planes ($X_1 = 0, X_2 = 0$, and $X_3 = 0$), i.e., the displacement component and the fluid flux in the direction normal to these planes are set to zero.



Figure 1: Cuboidal domain considered in the free-swelling boundary problem (a), and mechanically induced diffusion boundary value problem. Figures taken from [17, Figure 4 and 6].

	$\ r_k\ $	$\ r_k\ /\ r_0\ $
φ	10^{-9}	10^{-6}
\mathbf{J}_v	$5 * 10^{-12}$	10^{-9}

Table 1: Tolerances for the Newton-Raphson scheme. Here, r_k is the k -th residual. Table taken from [17, Table 3]

2.2.2 Mechanically induced diffusion boundary value problem

This problem was also investigated in [17]. Similar to the free-swelling boundary value problem, a cuboidal domain is also considered for the mechanically induced diffusion problem. However, here, zero Neumann boundary conditions for the normal component of the fluid flux are prescribed, while along the subset $(X_1, X_3) \in [-\frac{L}{3}, \frac{L}{3}] \times [-\frac{L}{3}, \frac{L}{3}]$ at the plane $X_2 = L$, highlighted in Figure 1(b), the coefficients of the displacement vector are prescribed as $u_i = [0, -\hat{u}, 0]$. Once again the intrinsic symmetry of the problem is exploited by specifying symmetry boundary conditions as described in section 2.2.1. The material parameters employed in the free energy function ψ and the dissipation potential ϕ are adopted from [17].

3 Implementation

In this paper, we use the implementation and setup from [17]. For the the finite element implementation of our model problem, we employed the `deal.II` software library [4] version 9.2.0. The MPI-parallel data distribution is handled using the `parallel::distributed::Triangulation`, which links to the external `p4est` library [6]. To solve the nonlinear system, we apply the Newton-Raphson scheme with the relative and absolute tolerances as provided in Table 1. For the parallel linear algebra, we use the `deal.II TrilinosWrappers` such that the `Trilinos` package `Epetra` is applied. Further, we use some functions implemented for standard tensor operations from [18]. The linearized system is solved using the Krylov iteration method GMRES. For GMRES, we use the parallel implementation provided by the `Trilinos` package `Belos` with a relative stopping criterion of $\|r_k\|/\|r_0\| \leq 10^{-8}$, where r_k is the k -th residual and r_0 the initial residual. `FROSch` is applied as a preconditioner. In all computations, we apply an algebraically computed overlap of two nodes ($\delta \approx 2h$) and employ the provided algebraic computation of the interface components. Applying `FROSch` in a completely algebraic sense implies using a one-dimensional null space. It has been shown that `FROSch` may be able to scale even if certain dimensions of the null space are neglected [13, 11]. However, this is not covered by the theory. A one-to-one correspondence between cores and subdomains is applied, and the global coarse problem is solved on a single core. We use `Trilinos` version 13.0.1 with small

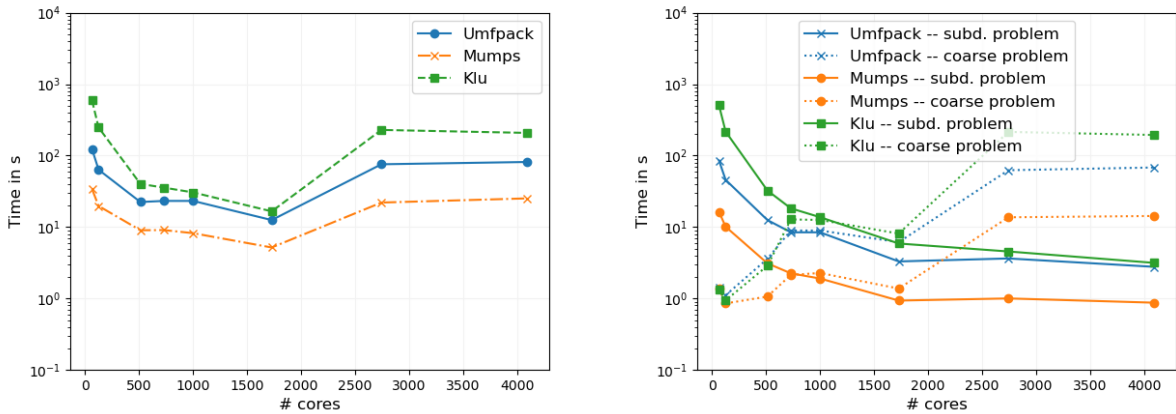


Figure 2: Strong scalability of the *solver time*, scaling from 64 to 4096 cores, for the linear elasticity model problem applying the FROSch preconditioner with th GDSW coarse space (left) and the detailed timers *subd. problem solve time* and the *coarse problem solve time* (right), including the time for the factorization and the forward./backward substitution. See Table 2 for the data.

modifications. We compare the performance of different sparse direct linear solvers, applying the build-in KLU solver from Amesos2 as well as Umfpack [7] and MUMPS [3] both interfaced through Amesos. We always use the same sparse solver for the local problems and the coarse problem. Using Trilinos version 13.0.1, we faced issues with the Amesos2 interfaces for Epetra matrices, such that we used the older Amesos interfaces in our tests; in more recent Trilinos versions, these issues may have been fixed. We use MUMPS in Version 5.6.0 without METIS, and Umfpack included in the Suite Sparse library Version 5.1.0, which uses METIS 5.1.0-IDX64. We consider the *solver time*, which denotes the time to build the preconditioner and to perform the Krylov iterations. The time to solve the subdomain problems as well as the time to solve the coarse problem includes the numerical factorization and the forward/backward substitution, denoted as *subd. problems solve time* and *coarse problem solve time*, respectively. For the *coarse problem solve time* the time is determined by lower level timers, such that it may deviate from the pure solution time by the sparse direct linear solver. All test were performed on the JSC supercomputer JUWELS [16] at the FZ Jülich using the Intel 2021.4.0 compiler and IntelMPI.

4 Numerical Results

4.1 Linear Elasticity

As a first example problem, we choose the linear elasticity model problem, described in section 2.1, using Q_1 finite elements on a structured mesh with 884 736 cells such that we have 2 738 019 degrees of freedom (DOF). Since we neglect the rotations from the null space, we may expect the number of iterations to increase with an increasing number of cores. For our tests, the number of iterations increases from 56 to 90 scaling from 64 to 4096 cores; see Table 2. Note that it has shown that the majority of the *solver time* is taken by the construction of the preconditioner rather than by the Krylov iterations for a smaller number of cores [17]. For this reason, the number of iterations should not influence the *solver time* significantly compared to the sizes of the subdomain problems within the considered range of cores.

linear elasticity – GDSW												
				solver time			subd. problems solve time			coarse problem solve time		
# cores	Krylov it.	max. size K_i	size K_0	Amesos		Amesos2	Amesos		Amesos2	Amesos		Amesos2
				MUMPS	Umfpack	KLU	MUMPS	Umfpack	KLU	MUMPS	Umfpack	KLU
64	56	86 577	932	34.04s	123.38 s	592.77 s	16.36 s	85.23 s	505.00 s	1.36 s	1.44 s	1.34 s
125	62	54 396	2 108	19.72s	63.39 s	246.96 s	10.11 s	45.80 s	217.09 s	0.85 s	1.11 s	0.94 s
512	72	21 504	10 412	9.02s	22.41 s	40.16 s	3.11 s	12.54 s	32.50 s	1.07 s	3.59 s	2.87 s
729	73	17 868	16 412	9.07s	23.21 s	35.64 s	2.25 s	8.44 s	18.27 s	2.14 s	8.95 s	12.79 s
1 000	78	14 724	20 037	8.21s	23.21 s	30.54 s	1.90 s	8.44 s	13.74 s	2.28 s	8.95 s	12.56 s
1 728	68	7 581	18 788	5.18s	12.53 s	16.58 s	0.94 s	3.30 s	5.88 s	1.38 s	6.14 s	8.10 s
2 744	86	8 700	60 090	22.02s	75.62 s	228.62 s	1.00 s	3.64 s	4.55 s	13.69 s	62.47 s	214.63 s
4 096	90	7 038	78 653	25.20s	81.41 s	207.76 s	0.87 s	2.77 s	3.15 s	14.29 s	68.19 s	194.30 s

Table 2: Strong scalability results for the linear elasticity model problem using Q_1 elements. We apply the FROSch preconditioner with the GDSW coarse space and an algebraic overlap of two elements and compare different sparse direct linear solver. The *solver time* is the time to build the preconditioner and to perform the Krylov iterations. The problem size is 2 738 019.

free-swelling problem – GDSW									
solver time									
# cores	avg. Krylov	$Q_1 Q_1$			$Q_1 RT_0$			avg. Krylov	Amesos2
		MUMPS	Umfpack	KLU	MUMPS	Umfpack	KLU		
64	70.9	173.24 s	536.41 s	1 587.04 s	49.7	75.35 s	238.57 s	686.13 s	
125	79.8	121.68 s	362.16 s	833.82 s	56.4	53.18 s	155.20 s	352.30 s	
512	103.4	71.88 s	213.51 s	250.88 s	73.7	41.18 s	122.68 s	134.44 s	
729	111.0	78.86 s	258.50 s	240.84 s	78.3	54.20 s	178.32 s	200.62 s	
1 000	116.3	73.49 s	241.98 s	216.39 s	81.3	53.48 s	167.36 s	154.35 s	
1 728	105.1	57.20 s	190.70 s	171.00 s	76.5	38.76 s	121.18 s	128.17 s	
2 744	125.1	147.99 s	599.51 s	1 068.12 s	86.8	172.00 s	646.72 s	1 547.63 s	
4 096	131.9	178.61 s	755.28 s	1 428.17 s	92.3	197.48 s	836.19 s	1 428.17 s	

Table 3: Strong scalability results for the free-swelling model problem. We apply the FROSch preconditioner with the GDSW coarse space and an algebraic overlap of two elements and compare different sparse direct linear solver. The *solver time* is the time to build the preconditioner and to perform the Krylov iterations. The problem size is 705 894 for $Q_1 Q_1$ elements and 691 635 for $Q_1 RT_0$ elements.

We obtain good strong scalability results scaling from 64 to 1 728 cores for all sparse direct linear solvers with MUMPS being the fastest. Umfpack is faster than KLU, however for smaller subdomain problem sizes (obtained from 729 to 1 728 cores) the results are comparable; see Table 2 and Figure 2. Reaching 2 744 cores the *solver time* starts to increase instead of decreasing. The reason for that is the significant increase for the size of the coarse problem, e.g., for 1 728 $\dim(K_0) = 18 788$ which compares to $\dim(K_0) = 60 090$ for 2 744 cores; see Table 2. From 2 744 cores on, the problem size relation of K_0 and max K_i is similar to 125 cores, where the *subd. problem solve time* dominated the *solver time*. The coarse problem reaches a critical size beyond 1 728 cores, since after this point the solution of the coarse problem begins to dominate the *solver time*; see Figure 2. The solution on a single core is not sufficient anymore. As a next step, we could apply three-levels or/and RGDSW. We want to remark that for certain numbers of cores and numbers of elements the decomposition obtained from *p4est* results in structured decompositions decreasing the size of the coarse problem. The proportion of the number of elements and the number of subdomains is decisive for this phenomenon.

4.2 Free-swelling boundary value problem

For the model problem described in section 2.2.1, we consider a mesh with 110 592 cells. We compare two types of ansatz functions for the flux field Q_1 and RT_0 , and for the deformation

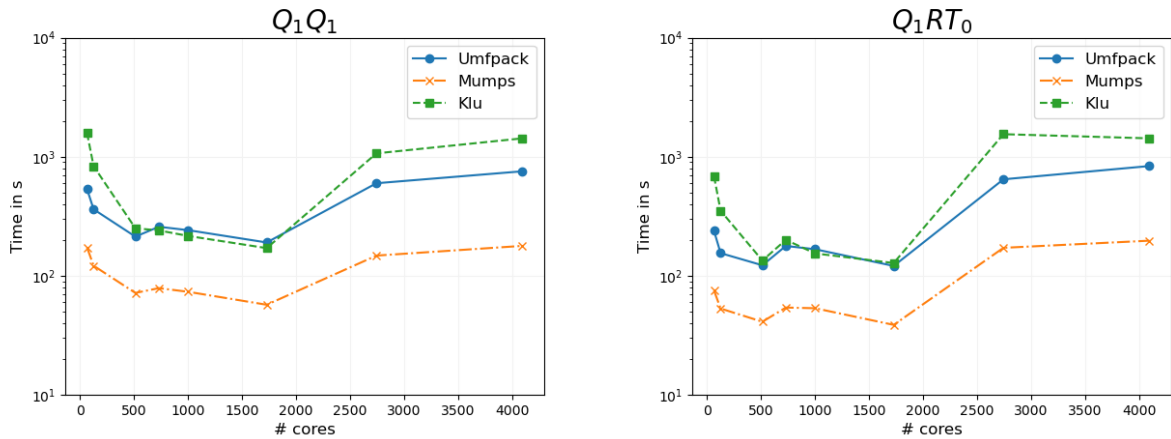


Figure 3: *solver time* scaling from 64 to 4096 cores using different direct linear solvers for the subd. problems of the FROSch preconditioner with a GDSW coarse space. The preconditioner is applied the *free-swelling* model problem. See Table 3 for the data.

field, we always use Q_1 elements. For Q_1Q_1 , we obtain 705 894 DOF and 691 635 DOF for Q_1RT_0 . We restrict the computation to two time steps. Each requires five Newton iterations. We take the *solver time* over the two time steps, such that the preconditioner is applied ten times. We consider an average number of Krylov iterations (*avg. Krylov*) over the ten Newton steps. Since we apply FROSch fully algebraically, i.e., using the null space of the Laplace operator for the construction of the coarse space, we cannot expect numerical scalability. Consequently, *avg. Krylov* increases with the number of cores; see Table 3.

Generally, the number of Krylov iterations is lower for the Q_1RT_0 elements, yet the increase from 64 to 4096 cores stronger than for the Q_1Q_1 elements. This is in agreement with the results obtained in [17]. Further, the size of the coarse problem is much larger with increasing number of cores. For 4096 cores, we obtain a coarse space dimension of 48 232 for Q_1Q_1 elements respectively 77 222 for Q_1RT_0 elements; see also Table 4. This indicates that the algebraic decomposition for the Q_1Q_1 is favorable since less interface components are obtained.

Regarding the strong scalability, we obtain similar results as for the linear elasticity model problem; compare Figures 2 and 3. For both ansatz functions, the *solver time* increases reaching 2 744 cores. The Q_1RT_0 elements are faster up to 1 728 cores. For larger number of cores the *solve coarse problem time* dominates the *solver time*. As previously discussed, the size of the coarse problem is smaller for Q_1Q_1 elements such that the *solver time* is faster for these elements employing larger numbers of cores. As for linear elasticity, the best performance of the solver framework is obtained using MUMPS. For 64 cores, MUMPS is more than 15 times faster than KLU and more than five times faster than Umfpack; see Table 3. The advantage of using MUMPS is most apparent if the size of the directly solved problem is large. From 1 728 to 4096 the *subd. problem solve time* Umfpack and KLU perform similarly, e.g., considering 1 728 cores, the time to solve the K_i s is 51.02s for Umfpack and 50.89s for KLU using Q_1Q_1 elements; see also Table 4 and Figure 4. Generally for smaller subdomain problem sizes Umfpack and KLU are comparable.

Although MUMPS is much faster than Umfpack and KLU the scalability is not extended solely by this choice of the direct linear solver.

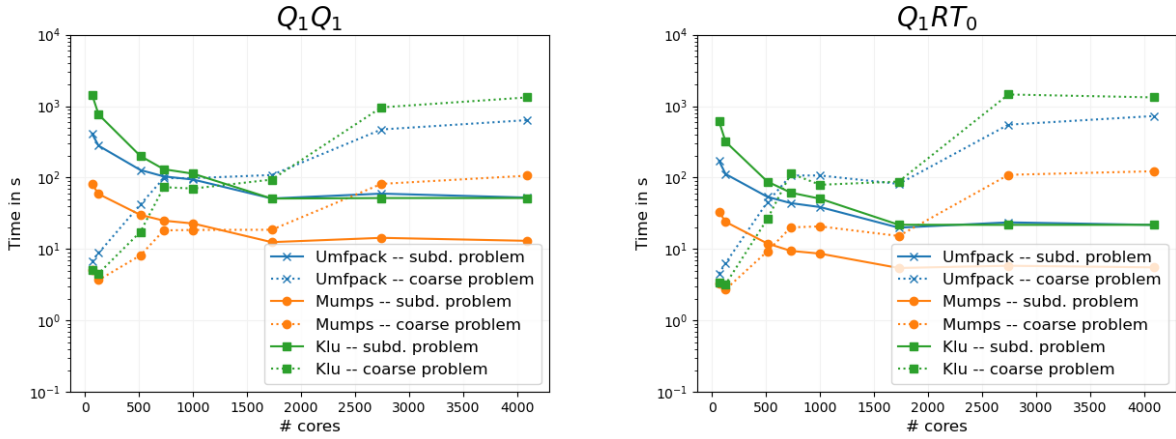


Figure 4: Time to solve the local subd. problems scaling from 64 to 4096 cores using different direct linear. See Table 4 for the data.

4.3 Mechanically induced diffusion problem

The results for the mechanically induced diffusion problem, introduced in section 2.2.2, confirm the results obtained for the free-swelling boundary value problem. Here, we also restrict the computation to two timesteps each solved with five Newton iterations. The more complex boundary conditions result in higher numbers of Krylov iterations. As for the other model problems, the number of iterations increases with an increasing number of cores. Yet, the change of boundary conditions does not affect the domain decomposition, such that the sizes for the subdomain problems K_i and the coarse problem K_0 are equal. Therefore, the strong scaling behavior is similar to the free-swelling problem; see Table 5. Consequently, for these tests, the *solver time* obtained using MUMPS is the fastest as well. The results comparing Umfpack and KLU for this model problem are remarkable. From 512 to 1728 cores the *solver time* using KLU is slightly faster than Umfpack, although it has been slower for the *free-swelling model problem*. The time to solve the subdomain problems again dominates *solver time* scaling from 64 to 1000 cores; see Tables 5 and 6 and Figures 5 and 6.

free-swelling problem – GDSW								
$Q_1 Q_1$					$Q_1 RT_0$			
subd. problem solve time								
	max. size K_i	Amesos		Amesos2		Amesos		Amesos2
		MUMPS	Umfpack	KLU	max. size K_i	MUMPS	Umfpack	KLU
64	38 334	81.29 s	412.17 s	1 453.55 s	35 634	33.33 s	171.26 s	615.22 s
125	27 648	58.90 s	279.19 s	763.12 s	25 598	24.02 s	112.08 s	317.11 s
512	13 896	30.06 s	127.59 s	200.50 s	12 571	11.95 s	53.77 s	87.94 s
729	11 472	24.97 s	103.84 s	130.83 s	10 368	9.43 s	43.92 s	61.50 s
1000	10 452	22.79 s	93.92 s	113.40 s	9 369	8.63 s	38.68 s	50.62 s
1728	5 634	12.49 s	51.02 s	50.89 s	5 064	5.43 s	19.91 s	21.87 s
2744	7 020	14.35 s	59.66 s	51.74 s	6 209	5.84 s	23.64 s	21.81 s
4096	6 312	13.03 s	52.51 s	51.74 s	5 563	5.54 s	21.75 s	21.81 s
coarse problem solve time								
	size K_0	Amesos		Amesos2	Size K_0	Amesos		Amesos2
		MUMPS	Umfpack	KLU		MUMPS	Umfpack	KLU
64	981	5.07 s	6.74 s	5.16 s	981	3.35 s	4.53 s	3.39 s
125	2 003	3.69 s	8.80 s	4.56 s	2 125	2.72 s	6.35 s	3.22 s
512	8 614	8.16 s	42.14 s	17.41 s	10 748	9.30 s	45.55 s	26.41 s
729	13 552	18.24 s	98.23 s	73.48 s	16 712	20.11 s	107.02 s	114.12 s
1 000	15 904	18.51 s	98.23 s	70.23 s	20 578	20.76 s	107.02 s	79.36 s
1 728	18 788	18.62 s	108.68 s	93.77 s	18 788	15.24 s	81.61 s	87.93 s
2 744	37 229	81.63 s	471.65 s	961.46 s	57 308	109.34 s	550.39 s	1 456.04 s
4 096	48 232	106.39 s	637.60 s	1 325.53 s	77 222	122.81 s	727.94 s	1 325.53 s

Table 4: Strong scalability for the *subd. problem solve time* and the *coarse problem solve time* using different sparse direct linear solvers. The time includes the factorization of problem and the forward./backw. substitution during the Krylov iterations. For the whole *solver time* see Table 3

mechanically-induced diffusion problem – GDSW								
solver time								
$Q_1 Q_1$					$Q_1 RT_0$			
# cores	avg.	Amesos		Amesos2	Avg.	Amesos		Amesos2
	Krylov	MUMPS	Umfpack	KLU	Krylov	MUMPS	Umfpack	KLU
64	115.8	214.14 s	739.30 s	1 654.99 s	119.9	113.30 s	432.78 s	753.36 s
125	130.0	154.23 s	500.88 s	887.11 s	137.2	85.14 s	300.36 s	399.83 s
512	177.2	100.06 s	323.04 s	292.94 s	180.3	74.06 s	265.61 s	183.75 s
729	186.4	112.14 s	390.50 s	288.87 s	192.3	102.14 s	395.56 s	260.95 s
1 000	196.4	107.12 s	374.02 s	262.23 s	205.4	106.15 s	386.94 s	224.96 s
1 728	210.6	97.71 s	356.62 s	226.93 s	219.5	88.08 s	320.87 s	192.73 s
2 744	224.4	241.59 s	1 008.08 s	1 212.64 s	235.6	362.65 s	1 561.48 s	1 846.48 s
4 096	239.1	295.22 s	1 283.16 s	1 606.95 s	249.0	422.36 s	2 027.79 s	2 372.35 s

Table 5: Strong scalability results for the *mechanically-induced diffusion* model problem. We apply the FROSch preconditioner with the GDSW coarse space and an algebraic overlap of two elements and compare different sparse direct linear solver. The *solver time* is the time to build the preconditioner and to perform the Krylov iterations. The problem size is 705 894 for $Q_1 Q_1$ elements and 691 635 for $Q_1 RT_0$ elements.

5 Conclusion

In our tests, we were able to reduce the *solver time* by over 80% with the choice of the sparse solver. We should therefore take particular interest in the choice of the solver using FROSch. For the considered model problems, we recommend using MUMPS since it performed the best. We expect a good performance of MUMPS for other model problems as well.

For the range of problems considered here, we did not face any memory issues with the direct solvers compared, and we did not specifically examine the memory usage. However, we expect differences in the range of possible subdomain and coarse problem sizes due to different memory demands of the different solvers.

mechanically induced diffusion problem – GDSW								
$Q_1 Q_1$					$Q_1 R T_0$			
subd. problem solve time								
	max. size	Amesos			max. size	Amesos		
	K_i	MUMPS	Umfpack	Amesos2 KLU	K_i	MUMPS	Umfpack	Amesos2 KLU
64	38 334	115.89 s	609.33 s	1 515.37 s	35 634	61.56 s	351.75 s	673.00 s
125	27 648	85.54 s	409.80 s	809.69 s	25 598	47.02 s	239.01 s	356.35 s
512	13 896	46.94 s	207.11 s	229.25 s	12 571	25.06 s	122.50 s	112.68 s
729	11 472	38.56 s	166.92 s	152.12 s	10 368	20.03 s	100.85 s	81.18 s
1 000	10 452	35.56 s	152.18 s	131.74 s	9 369	18.88 s	92.55 s	69.41 s
1 728	5 634	22.80 s	90.63 s	65.87 s	5 064	13.30 s	53.54 s	34.12 s
2 744	7 020	23.92 s	101.89 s	65.43 s	6 209	13.75 s	62.04 s	34.43 s
4 096	6 312	21.98 s	89.07 s	65.43 s	5 563	13.01 s	56.25 s	34.43 s
coarse problem solve time								
	max. size	Amesos			max. size	Amesos		
	K_i	MUMPS	Umfpack	Amesos2 KLU	K_i	MUMPS	Umfpack	Amesos2 KLU
64	981	5.32 s	7.92 s	5.42 s	981	4.36 s	7.18 s	4.43 s
125	2 003	4.25 s	12.21 s	5.34 s	2 125	4.06 s	13.04 s	5.08 s
512	8 614	11.64 s	68.46 s	22.99 s	10 748	16.23 s	103.86 s	38.81 s
729	13 552	25.86 s	167.40 s	87.50 s	16 712	35.08 s	239.38 s	132.98 s
1 000	15 904	26.73 s	167.40 s	85.64 s	20 578	38.30 s	239.38 s	107.88 s
1 728	18 788	30.67 s	206.60 s	116.33 s	18 788	31.65 s	218.03 s	117.71 s
2 744	37 229	119.86 s	788.58 s	1 059.76 s	57 308	204.04 s	1 315.37 s	1 633.51 s
4 096	48 232	156.47 s	1 076.23 s	1 432.02 s	77 222	233.64 s	1 748.85 s	2 130.84 s

Table 6: Strong scalability for the *subd. problem solve time* and the *coarse problem solve time* using different sparse direct linear solvers. The time includes the factorization of problem and the forward./backw. substitution during the Krylov iterations. For the whole *solver time* see Table 5

Acknowledgments

The authors acknowledge the DFG project 441509557 (<https://gepris.dfg.de/gepris/projekt/441509557>) within the Priority Program SPP2256 “Variational Methods for Predicting Complex Phenomena in Engineering Structures and Materials” of the Deutsche Forschungsgemeinschaft (DFG). The authors gratefully acknowledge the Gauss Centre for Supercomputing e.V. (www.gauss-centre.eu) for providing computing time on the GCS Supercomputer JUWELS [16] at the Jülich Supercomputing Centre (JSC) for the project *FE2TI - High performance computational homogenization software for multi-scale problems in solid mechanics*.

REFERENCES

- [1] Reference documentation for deal.II version 9.3.0 - the step-8 tutorial program., 2021.
- [2] Trilinos public git repository. Web, 2021.
- [3] P. Amestoy, A. Buttari, I. Duff, A. Guermouche, J.-Y. L’Excellent, and B. Uçar. Mumps. In D. Padua, editor, *Encyclopedia of Parallel Computing*, pages 1232–1238. Springer US, Boston, MA, 2011.
- [4] W. Bangerth, C. Burstedde, T. Heister, and M. Kronbichler. Algorithms and data structures for massively parallel generic adaptive finite element codes. *ACM Trans Math Softw*, 38(2):1–28, 2011.
- [5] L. Böger, A. Nateghi, and C. Miehe. A minimization principle for deformation-diffusion processes in polymeric hydrogels: Constitutive modeling and FE implementation. *Int J Solids Struct*, 121:257–274, 2017.

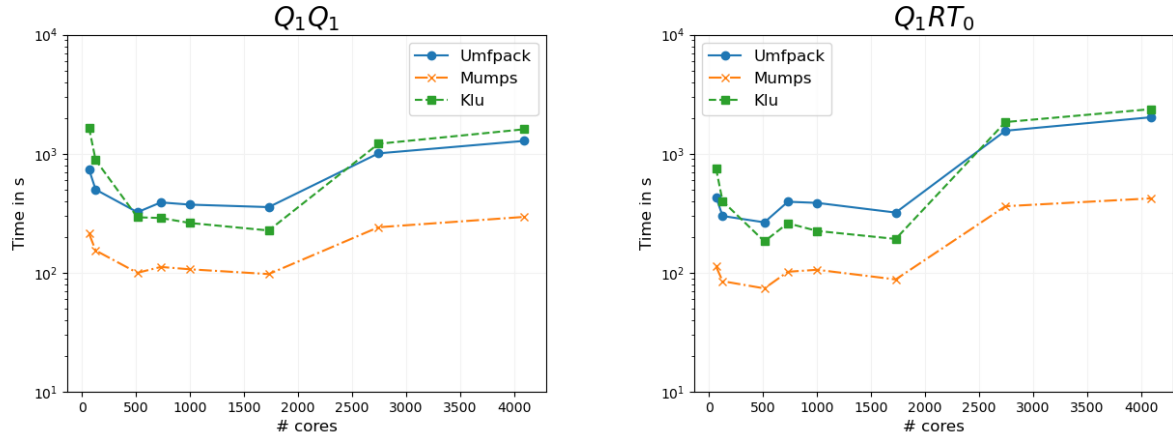


Figure 5: Solver time scaling from 64 to 4096 cores using different direct linear solvers for the subd. problems of the FROSch preconditioner with a GDSW coarse space. The preconditioner is applied the *mechanically induced diffusion* model problem. See Table 5 for the data.

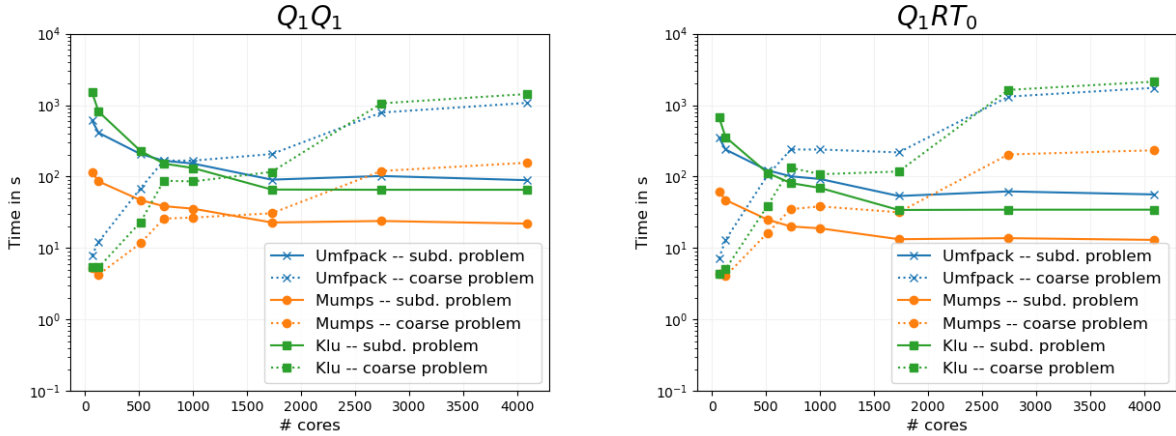


Figure 6: Time to solve the local subd. problems scaling from 64 to 4096 cores using different direct linear. See Table 6 for the data.

- [6] C. Burstedde, L. C. Wilcox, and O. Ghattas. `p4est`: Scalable algorithms for parallel adaptive mesh refinement on forests of octrees. *SIAM J Sci Comput*, 33(3):1103–1133, 2011.
- [7] T. A. Davis and I. S. Duff. A combined unifrontal/multifrontal method for unsymmetric sparse matrices. *ACM Trans Math Softw*, 25(1):1–20, 1999.
- [8] C. R. Dohrmann, A. Klawonn, and O. B. Widlund. Domain decomposition for less regular subdomains: Overlapping Schwarz in two dimensions. *SIAM J Numer Anal*, 46(4):2153–2168, 2008.
- [9] C. R. Dohrmann, A. Klawonn, and O. B. Widlund. A family of energy minimizing coarse spaces for overlapping Schwarz preconditioners. In *Domain decomposition methods in science and engineering XVII*, volume 60 of *LNCSE*. Springer, 2008.

- [10] C. R. Dohrmann and O. B. Widlund. On the design of small coarse spaces for domain decomposition algorithms. *SIAM J Sci Comput*, 39(4):A1466–A1488, 2017.
- [11] A. Heinlein, C. Hochmuth, and A. Klawonn. Fully algebraic two-level overlapping Schwarz preconditioners for elasticity problems. In F. Vermolen and C. Vuik, editors, *Numerical Mathematics and Advanced Applications ENUMATH 2019*, pages 531–539, Cham, 2021. Springer International Publishing.
- [12] A. Heinlein, A. Klawonn, S. Rajamanickam, and O. Rheinbach. FROSch: A fast and robust overlapping Schwarz domain decomposition preconditioner based on Xpetra in Trilinos. In R. Haynes, S. MacLachlan, X.-C. Cai, L. Halpern, H. H. Kim, A. Klawonn, and O. Widlund, editors, *Domain Decomposition Methods in Science and Engineering XXV*, pages 176–184, Cham, 2020. Springer.
- [13] A. Heinlein, A. Klawonn, and O. Rheinbach. A parallel implementation of a two-level overlapping Schwarz method with energy-minimizing coarse space based on Trilinos. *SIAM J Sci Comput*, 38(6):C713–C747, 2016.
- [14] A. Heinlein, O. Rheinbach, and F. Röver. Parallel scalability of three-level FROSch preconditioners to 220 000 cores using the theta supercomputer. *SIAM J Sci Comput*, 45(3):S173–S198, 2023.
- [15] A. Heinlein, O. Rheinbach, F. Röver, S. Sandfeld, and D. Steinberger. Applying the FROSch overlapping Schwarz preconditioner to dislocation mechanics in deal.ii. *PAMM*, 19(1):e201900337, 2019.
- [16] Jülich Supercomputing Centre. JUWELS Cluster and Booster: Exascale Pathfinder with Modular Supercomputing Architecture at Juelich Supercomputing Centre. *Journal of large-scale research facilities*, 7(A138), 2021.
- [17] B. Kiefer, S. Prüger, O. Rheinbach, and F. Röver. Monolithic parallel overlapping Schwarz methods in fully-coupled nonlinear chemo-mechanics problems. *Comput Mech*, 71(4):765–788, 2023.
- [18] A. McBride, A. Javili, P. Steinmann, and B. D. Reddy. A finite element implementation of surface elasticity at finite strains using the deal.II library. *arXiv:1506.01361 [physics]*, June 2015.
- [19] A. Toselli and O. Widlund. *Domain decomposition methods—algorithms and theory*, volume 34 of *Springer Series in Computational Mathematics*. Springer-Verlag, Berlin, 2005.